

Molecular Hydrogen Formation During Dense Interstellar Cloud Collapse

Kinsuk Acharyya¹, Sandip K. Chakrabarti^{2,1} and Sonali Chakrabarti^{3,1}

¹ *Centre for Space Physics, Chalantika 43, Garia Station Rd., Kolkata, 700084, India*

² *S. N. Bose National Center for Basic Sciences, JD-Block, Salt Lake, Kolkata, 700098, India*

³ *Maharaja Manindra Chandra College, 20 Bhupen Bose Avenue, Kolkata 700003*

7 February 2020

ABSTRACT

We study the evolution of molecular hydrogen on the grain surfaces and in the gas phase using both the rate equation (which tracks the average number of molecules) and the master equation (which tracks the expectation values of molecules). We show that above a certain critical accretion rate of H on the grains, the results from these two methods become identical. We used this result to follow the collapse of a dense interstellar cloud and studied the formation of molecular hydrogen for two different temperatures ($T=10\text{K}$ and 12K) and two different masses ($1M_{\odot}$ and $10M_{\odot}$) of the cloud when olivine grains were used. Since at higher temperatures, the recombination is very small for these grains, we also studied a similar hydrodynamic processes at higher temperatures ($T=20\text{K}$ and 25K) when amorphous carbon grains were used. We find that generally, for olivine grains, more than 90% H is converted to H_2 within $\sim 10^{5-7}\text{yr}$ whereas for amorphous grains it takes $\sim 10^{6-7}\text{yr}$. H_2 formed in this manner can be adequate to produce the observed complex molecules.

SUBMITTED FOR PUBLICATION IN MNRAS

1 INTRODUCTION

Over the last few years several works have been carried out to investigate the formation of complex molecules in cool interstellar clouds (Prasad and Huntress 1980a, 1980b; Leung,

Herbst and Hübner 1984; Hasegawa and Herbst 1993, Hasegawa, Herbst and Leung 1992). One of the stumbling blocks has been to identify mechanisms to produce H_2 molecules. It is has been realized that purely gas phase reactions are so improbable that one needs to invoke the grain chemistry (e.g., Gould and Salpeter 1963; Hollenbach and Salpeter 1971; Hollenbach, Werner and Salpeter 1971). More recently, Biham et al. (2001), and Green et al. (2001) have computed H_2 production rate by physisorption. It was found that significant production is possible in cooler ($\sim 10 - 25\text{K}$) clouds (see, also, Stantcheva, Shematovich & Herbst 2002; Rae et al. 2003; Lipshtat et al. 2004). Subsequently, Cazaux & Tielens (2002, 2004) used both physisorption and chemisorption, especially to demonstrate that H_2 production is possible at high temperatures ($\sim 200 - 400\text{K}$), as well. In these works, the H atoms combine together on the surface of the grains to form H_2 and then they are desorbed into the gas phase to react with other atoms. Whereas the investigations have been made to generally understand the rate of such reactions in presence of constant accretion rate of H onto the grain surface, and perhaps with a single type of grains, one requires to investigate this problem afresh in a realistic situation of collapse of dense proto-stellar clouds where accretion rates may vary in the presence of a grain size distribution.

In the first paper of this series, we investigate precisely this problem. For concreteness, we concentrate on cool, dense interstellar clouds. We assume typical stationary models of proto-stellar collapse of these clouds and compute the formation of H_2 molecules as the flow collapses. For number and size distributions of grains, we use the standard models of the grains (suitable for dense clouds) present in the literature. As far as the grain-surface chemistry goes, we compute using both the rate equation approach (e.g., Hasegawa, Herbst and Leung 1992) as well as the master equation (probabilistic) approach (e.g., Biham et al. 2001, Green et al. 2001). The rate equation deals with the variation of the number density of the particles and probabilistic equation deals with the expectation value of the hydrogen number density. By comparing the H_2 formation in two methods, we conclude that the results of these approaches become identical at extremely small accretion rate as well as at large accretion rate $F_H > F_{H,c}$, where the exact value of the *critical accretion rate* $F_{H,c}$ depends on the grain size. (For definition of F_H , see, Eq. 9 below.) Typically, as we show in Sec. 2.4, $F_{H,c} \sim 0.1 - 2/\text{s}$. For grains of smaller size, $F_{H,c}$ is larger, i.e., rate equations can be used if the accretion rate is sufficiently large. The first procedure is computationally faster and is valid when the average number of each species on the grain is high. The second procedure is slower and is useful when the average number of species is low. In a realistic

collapse, the value of $F_{H,c}$ depends on the effective area of the grains, i.e., the sum of all the grain surfaces. After following such self-consistent procedures, we conclude that a significant H_2 is formed in the cloud during the collapse. Since H_2 is a precursor of more complex bio-molecules, we believe that future works on bio-molecule formation based on our present results would be more reliable.

The plan of the present paper is the following: In §2, we discuss the grain size distribution in a cloud. We also discuss the rate and the master equations. We show that the contribution of small grains towards the grain chemistry is more significant since their number density is much higher. We first compute recombination efficiency $2R_{H_2}/F_H$ (Biham et al. 2001) as a function of temperature for two different activation barrier energies in order to select the suitable temperature range in which H_2 formation could become significant in the cold cloud condition. We compare the results $H + H \rightarrow H_2$ on grains using both the rate equation and master equation approaches as a function of accretion rate of H and show that at high and very low rates, the results from these two approaches merge. In §3.1, we first discuss our results for the case when the cloud is static, i.e., each shell starting with the same initial condition. We consider the cloud of high and low mass and of two different temperatures. We then show the variations of H and H_2 as functions of the radial co-ordinate. Since the cloud parameters are not very accurately known, we carry out the procedure for the cloud temperatures $T = 10\text{K}$ and $T = 11\text{K}$ respectively, as appropriate for a cold, dense cloud. In §3.2, we consider collapse of spherical shells. Here, the number densities are high, and thus the formation of H_2 on the grains and the subsequent desorption of H_2 to the gas are significant. We chose two types of grains such as olivine (at 10 and 12K) and amorphous carbons (20 and 25K respectively) and use corresponding activation barrier energies. Finally, in §4, we make concluding remarks.

2 CLOUD AND GRAIN PROPERTIES

2.1 Cloud Properties

A generic interstellar cloud may have several distinct regions (e.g., van Dishoeck et al. 1993). Diffused clouds have typical number density $\sim 100-800\text{cm}^{-3}$ and temperature $T \sim 30-80\text{K}$ and a mass could vary from $1M_\odot$ to $100M_\odot$. Translucent clouds are in the similar mass range, but have number density $\sim 500-5000\text{cm}^{-3}$ with a bit lower temperature (15–50K). Cold dark clouds have temperatures around 10–25K, but the number densities are much

higher ($10 - 10^4 \text{cm}^{-3}$) and the corresponding masses can vary from $0.3 - 10 M_\odot$ at the core to $10 - 10^3 M_\odot$ at the cloud region. In terms of extinction parameter R_v , it appears that a diffused cloud has $R_v \sim 3.1$, an intermediate dense region has $R_v \sim 4.0$ and a dense cloud has $R_v \sim 5.5$ (Weingartner & Draine, 2001a). In contrast, the giant molecular clouds will have densities around 300cm^{-3} at the outer complex, $10^2 - 10^4 \text{cm}^{-3}$ at the clouds, $10^4 - 10^7 \text{cm}^{-3}$ in the warm regions while $10^7 - 10^9 \text{cm}^{-3}$ in the hot cores. The typical size of a molecular cloud is around a parsec or so with an average lifetime $\sim 10 - 20$ Myr. In the outer regions, the cloud may pass through an isothermal phase where the temperature is constant. Heat generated in this phase is radiated away through the optically thin region. As the cloud collapses, the radiation is trapped due to the high optical depth and the gas becomes more adiabatic (Hartmann 1998). Though our numerical approach is capable of handling temperature variation inside a cloud, in the absence of a suitable and satisfactory distribution, in the present work, we shall consider the clouds of constant temperatures for the sake of simplicity.

2.2 Size Distribution of Grains

A small fraction (in terms of the number density) of the interstellar cloud is in the form of dusts and grains. These grains play an important role in the formation of stars and planetary systems and in our context, causing chemical evolution of molecules. The degree of importance of the dust depends on the ratio of the number density of grains to gas atoms or molecules at each radius. Here we discuss two models of grains which we follow:

(a) MRN model:

The simplest model which can reproduce functional dependence of the extinction with wavelength is due to Mathis, Rumpl and Nordsieck (1977). According to this so-called MRN model, the number density of grains having size between a to $a + da$ is given by,

$$dn_{gr} = C n_H a^{-3.5} da, \quad a_{min} < a < a_{max}, \quad (1)$$

where, n_H is the number density of hydrogen, a is the grain-radius in cm . This relation is strictly valid between the minimum and the maximum size of the grains $a_{min} = 50 \text{ \AA}$ and $a_{max} = 2500 \text{ \AA}$. The grain constant, taken from Draine and Lee (1984) is given by $C = 10^{-25.13}$.

(b) Weingartner and Draine (WD) model:

Weingartner and Draine (2001b, hereafter WD01) revised the MRN distribution for the

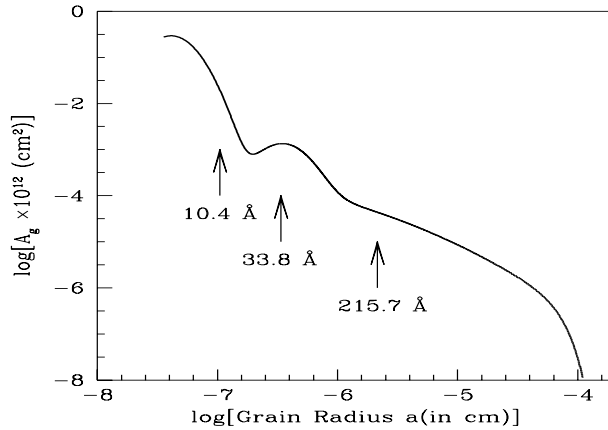


Fig. 1: Variation of the effective grain area A_g as a function of the grain radius indicating that smaller grains have the highest contribution. Instead of choosing continuous distribution, three types of ‘average’ grains have been assumed having radii 10.4 Angstrom (type 1), 33.8 Angstrom (type 2) and 215.7 Angstrom (type 3) respectively which have the same total number of grains. The arrows are drawn at humps of the Weingartner & Draine (2001b) distribution function.

entire range of grain size which is applicable to Milky way, LMC and SMC. This revision was needed to incorporate the real interstellar environment through which starlight passes. The parameters include reddening and carbon abundances. For instance, when the carbon abundance is negligible, this distribution becomes close to the MRN distribution. This distribution is valid for grains with $a > 3.5$ Angstrom. If we take the weighted surface area (i.e., surface area of the grain $\propto a^2$) multiplied by the number-density, that would give the effective surface area per unit volume contributed by the grains of a given size a . In Fig. 1, we present this plot for the parameters suitable for dense interstellar cloud ($R_v^b = 5.5$ and Case A from Table 1 of WD) used in the WD distribution. It is clear that the small sized grains contribute the most because of their large number density. It is also clear that there are three sizes of grains which are important: (a) smallest one with $a \sim 10$ Angstrom (Type 1), (b) the intermediate one with $a \sim 35$ Angstrom (Type 2) and (c) large grains with $a \sim 200$ Angstrom (Type 3). The actual values, marked by arrows have been computed from the humps in the WD distribution. For simplicity of computation of the accretion rate on each type of grain and their catalytic effect, we assume that only these three types of grains exist. Their number densities are estimated self-consistently from area under the curve given by WD distribution. See, Acharyya, Chakrabarti & Chakrabarti (2002, 2004) for application of this considerations.

2.3 Equations governing the formation of molecular hydrogen

(a) Rate equation method

Where the grain has large number of reactant atoms or molecules, it is convenient to use this method. Here one deals with the average number of reactants.

Let us consider n_H to be the number of H atoms on a grain at time t and let n_{H_2} be the number of H_2 molecules at that instant, then the following equation gives the rate at which number density of H changes:

$$\frac{dn_H}{dt} = F_H - W_H n_H - 2(A_H/S)n_H^2. \quad (2a)$$

Here, F_H is the accretion rate of H which increases the number of H on a grain by sticking to it. W_H is the desorption co-efficient of hydrogen $= \nu \exp(-E_1/k_b T)$, where, E_1 is the activation barrier energy for desorption of H atom, k_b is the Boltzmann's constant and T is the temperature of the grain, assumed to be the same as the gas. Since in our case the number density is high $\sim 10^4 \text{ cm}^{-3}$ and above, such an assumption is justified. The second term causes a reduction of the number of hydrogen atoms on the grain, hence the minus sign. On the grain surface, mainly due to diffusive processes, two H atoms combine to form a single H_2 molecule. $A_H = \nu \exp(-E_0/k_b T)$, the hopping rate, gives the probability of this to happen. Here, ν is the vibrational frequency,

$$\nu = \frac{2sE_d}{\pi^2 m_H} \quad (2b)$$

where, $s \sim 10^{14}$ is surface density of sites on a grain (Biham, 2001), m_H is the mass of the H atom and E_d is the binding energy. This is normally taken to be $10^{12} - 10^{13} s^{-1}$. E_0 is the activation barrier energy for diffusion of H atom. This term also reduces the number of H and hence the minus sign in the equation. The diffusion through tunneling has not been taken into account as it could be less important (Katz et al. 1999). S is the number of sites per grain:

$$S = 4\pi r^2 s. \quad (2c)$$

It may be relevant to discuss the nature of the third term of Eq. (2a). If the fraction f_{gr} of grain-sites occupied by any of the species is very small ($f_{gr} \ll 1$), then in order to form an H_2 , the incoming H has to hop, on an average S times to combine with another H located at an average distance of $S^{1/2}$ through a well known 'random-walk' process. This accounts for the factor S in the third term which effectively reduces the diffusion rate. However, as f_{gr} becomes significant, any direction that the incoming H hops to would be useful for forming

an H_2 and thus the factor may be reduced to $S^{1/2}$ or even less instead of S . In the present circumstance, f_{gr} is indeed very small and we use the factor S in the denominator as in Biham et al. (2001) or Lipshtat et al. (2004).

The following equation gives the rate at which the number density of H_2 increases with time:

$$\frac{dn_{H_2}}{dt} = 2\mu(A_H/S)n_H^2 - W_{H_2}n_{H_2}, \quad (2d)$$

where, W_{H_2} is the desorption co-efficient of hydrogen molecule given by $\nu \exp(-E_2/k_bT)$, E_2 is the activation barrier energy for desorption of H_2 molecule. The parameter μ represents the fraction of H_2 molecule that remains on the surface upon formation while $(1-\mu)$ fraction is desorbed spontaneously due to the energy released in the recombination process. The H_2 production rate R_{H_2} in the gas due to grain is then given by,

$$R_{H_2} = (1 - \mu)(A_H/S)n_H^2 + W_{H_2}n_{H_2}. \quad (3)$$

However, the net production rate in the gas phase is obtained by inclusion of the breakdown of H_2 by cosmic rays, the rate of which is assumed to be 10^{-17} s^{-1} (Millar et al. 1997). The values for energy barriers E_0 , E_1 , E_2 and μ are taken from Katz et al. (1999). In our calculations, we used $E_0 = 24.7 \text{ meV}$, $E_1 = 32.1 \text{ meV}$, $E_2 = 27.1 \text{ meV}$ and $\mu = 0.33$ for olivine and $E_0 = 44 \text{ meV}$, $E_1 = 46.7 \text{ meV}$, $E_2 = 46.7 \text{ meV}$ and $\mu = 0.413$ for amorphous carbon grains. Because of the difference in barrier energy, the recombination efficiencies (defined as $\eta = 2R_{H_2}/F_H$, see, Biham et al. 2001) are high at completely different temperature ranges. In Fig. 2(a-b), we show η for (a) olivine and (b) amorphous carbon computed using the rate equation. Here we also included the Langmuir & Hinshelwood rejection term which rejects the accretion of H and H_2 in the occupied sites. This term essentially reduces the efficiency at lower temperature. The curves are drawn for three accretion rates $F_H = 10^{-8} \text{ s}^{-1}$ (solid), 10^{-6} s^{-1} (dotted) and 10^{-4} s^{-1} (dashed) respectively which are appropriate for the dense clouds considered in this paper. It is to be noted that for olivine (Fig. 2a), the useful temperature range is around $7 - 13 \text{ K}$ and for carbon (Fig. 2b), this range is around $13 - 25 \text{ K}$. We therefore select the low cloud temperatures ($T = 10$ and 12 K) for the first case and relatively higher temperatures ($T = 20$ and 25 K) for the second case. One could imagine having unusually high accretion rates in dense clouds which might allow H_2 production at even higher temperatures where η is still significant.

(b) Master Equation Method

It is convenient to use the master equation method (Biham et.al. 2001) to study the

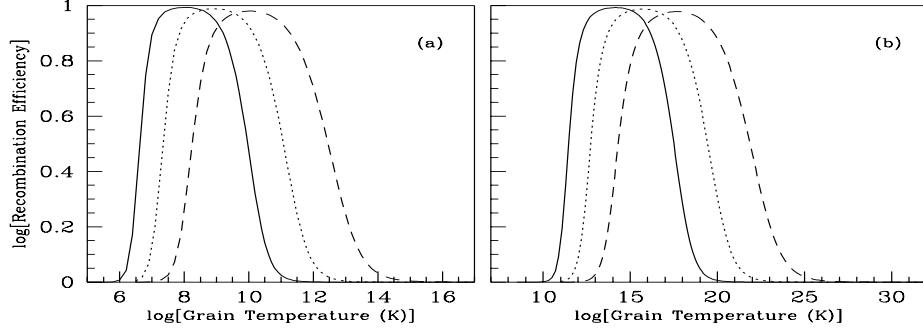


Fig. 2: Variation of recombination efficiency η as a function of the grain temperature in (a) olivine and (b) amorphous carbon respectively. The solid, dotted and dashed curves are drawn for $F_H = 10^{-8} s^{-1}$, $10^{-6} s^{-1}$ and $10^{-4} s^{-1}$ respectively.

formation process when the number of species in the grain is ‘small’. This process accounts for both the discrete nature of the hydrogen and the fluctuations and solves the problem probabilistically. For instance, its dynamical variables are the probability $P_H(N_H)$ that there are N_H atoms on a grain at a given time. One needs to study the time evolution of the probabilities through the same type of equations as in Eq. 2(a-b), except that the expectation values $\langle N_H \rangle$ and $\langle N_{H_2} \rangle$ are to be used instead of the average density. **The equations are:**

$$\frac{d \langle N_H \rangle}{dt} = F_H - W_H \langle N_H \rangle - 2(A_H/S) \langle N_H(N_H - 1) \rangle, \quad (4a)$$

and

$$\frac{d \langle N_{H_2} \rangle}{dt} = \mu(A_H/S) \langle N_H(N_H - 1) \rangle - W_{H_2} \langle N_{H_2} \rangle. \quad (4b)$$

Since $P_H(N_H)$ represents the probability that there are N_H hydrogen atoms on the grain, by sum rule on probabilities:

$$\sum_{N_H=0}^{\infty} P_H(N_H) = 1. \quad (5)$$

The time derivatives of these probabilities, $\dot{P}_H(N_H)$ are given by (Biham et al. 2001),

$$\begin{aligned} \dot{P}_H(N_H) = & F_H[P_H(N_H - 1) - P_H(N_H)] + W_H[(N_H + 1)P_H(N_H + 1) - N_H P_H(N_H)] + \\ & + (A_H/S)[(N_H + 2)(N_H + 1)P_H(N_H + 2) - N_H(N_H - 1)P_H(N_H)]. \end{aligned} \quad (6a)$$

Similarly, the probability that there are N_{H_2} hydrogen molecules on the grain is given by $P_{H_2}(N_{H_2})$. **The time evolution of these probabilities is given by,**

$$\dot{P}_{H_2}(N_{H_2}) = W_{H_2}[(N_{H_2} + 1)P_{H_2}(N_{H_2} + 1) - N_{H_2}P_{H_2}(N_{H_2})]$$

$$+\mu(A_H/S) < N_H(N_H - 1) > [P_{H_2}(N_{H_2}) - P_{H_2}(N_{H_2} - 1)]. \quad (6b)$$

Note that the last term in Eq. 6b, does not exactly correspond to the last term in Eq. (13) of Biham et al. (2001). Perhaps there was a typographical error in the latter equation.

From these probabilities, one gets the expectation values for the number of H atoms on the grain as,

$$< N_H > = \sum_{N_H=0}^{\infty} N_H P_H(N_H), \quad (7a)$$

and the rate of formation of hydrogen molecules on the surface is,

$$< N_{H_2} > = A_H \sum_{N_H=2}^{\infty} N_H(N_H - 1) P_H(N_H). \quad (7b)$$

The number of hydrogen molecules which are released back into the gas is given by,

$$R_{H_2} = (1 - \mu)(A_H/S) < N_H(N_H - 1) > + W_{H_2} < N_{H_2} > . \quad (8)$$

2.4 Regime of Interest for Self-consistent Study

Before we study the molecular hydrogen formation in a collapsing cloud, we like to enquire if the rate equation or the master equation is to be used for time evolution. For these, we require the accretion rate of H falling on a given grain. We compute three accretion rates for three different sizes of the grains.

As in the kinetic theory, the accretion rate is computed from the rate of H which a grain ‘sees’. This is given by,

$$F_H = \alpha \pi r^2 V n_h, \quad (9)$$

where, α is the probability that a H atom will stick to a grain, V is the root mean square velocity of the hydrogen which is given by,

$$V = \sqrt{8k_b T / \pi m_p}, \quad (10)$$

n_h is the number density of hydrogen, r is the mean radius of a grain r_{grain} . More accurately, it is the sum of the radii of the grain and the hydrogen atom. So we use, $r = r_{grain} + r_H$ ($r_H \sim 10^{-8}$ cm is the radius of a hydrogen atom). α may vary from 0.1 to 1. We use $\alpha = 0.5$ throughout the paper. m_p is the mass of an hydrogen atom. (van Dishoeck et al. 1993).

Figure 3 gives the time evolution of the variation of the number of H and H_2 on a grain surface at a given accretion rate of H for the small grains (Type 1) using both the

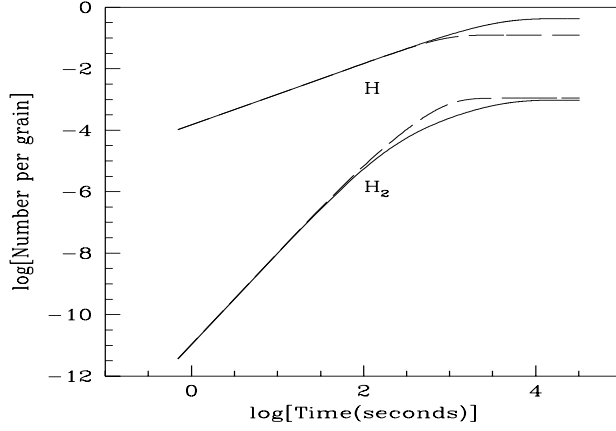


Fig. 3: Time evolution of the H and H_2 numbers per grain using the average method, i.e., using the rate equation (long dashed curve) and the probabilistic method, i.e., using the master equation (solid curve). The saturation takes place in less than a day.

rate equation (long dashed) and the master equation (solid curve). We choose the gas/grain temperature to be 10 K. The accretion rate has been chosen to be 1.5×10^{-4} . Note that within about 10^4 s, both H and H_2 saturate. This time is negligible compared to the infall time. Thus, in our computation in future, we assume that H and H_2 saturate instantaneously.

In Figs. 4(a-b) we plot these saturation values for all three types of grains as functions of accretion rate of H when the gas/grain temperature is 10K. In Fig. 4(a), we compare the number of H for all three types of grains (marked) obtained from the rate (long dashed) and from the master (solid curves) equations. Note that for extremely low value of the accretion rate, these two methods are close to each other. For sufficiently high rate, these two values merge. For lower rate, the results from the master equation is independent of the grain size. If Fig. 4(b), we draw similar curves for the saturated values of H_2 . The rate equation gives different saturation values for different types of grains (marked) while the master equation gives virtually similar values. Because in both the Figs. 4(a-b), the rate and master equations roughly merge above the accretion rate of $F_{H,c} \sim 2s^{-1}$, in our computation of H_2 formation during cloud collapse, we shall assume that when the rate is smaller than $2s^{-1}$, the master equation should be used, and if it is larger than $2s^{-1}$, the rate equation should be used. This is therefore a model-independent description and can be used even for time dependent work. We performed similar computations in various temperatures and found the trend of the results to be similar.

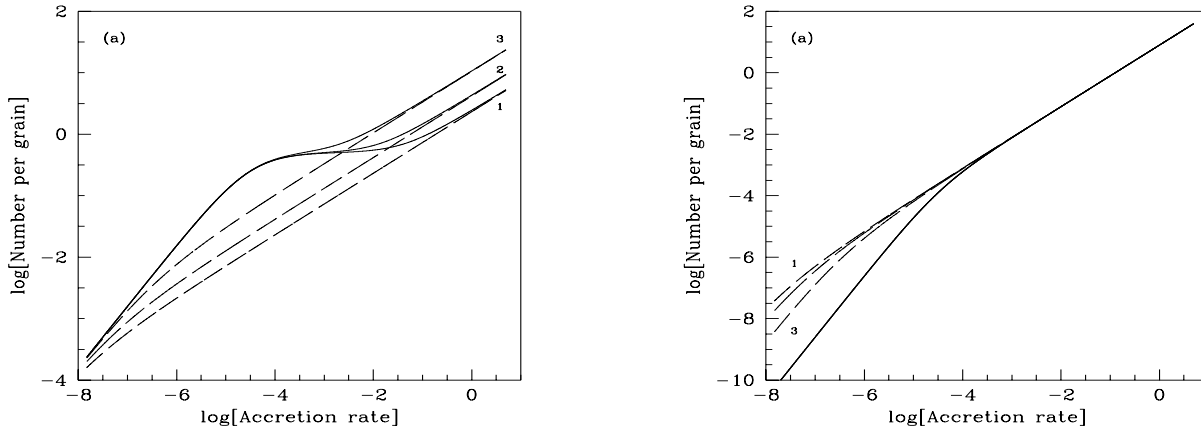


Fig. 4(a-b): Variation of the saturation values of the number of (a) H and (b) H_2 as a function of the accretion rate of hydrogen on different types of grain surfaces (marked) when the gas/grain temperature is 10K. Both the rate equation (long dashed curves) and master equation (solid curves) have been used. In (a), the number of H is the same from both the equations as very low and high rates. In (b), only at high rates the rates are similar. This shows that above a critical accretion rate of $\sim 1s^{-1}$ rate equations could be used for the production of H_2 .

3 CLOUD COLLAPSE AND H_2 FORMATION

So far, we presented the way the H_2 formation should be computed in presence of a size-distribution of grains. We showed in particular that when the accretion rate is higher than certain value either the rate equation or the master equation could be used, though it is computationally faster to use the rate equation approach. In lower rates, only the master equation approach or the probabilistic approach should be used. We now apply our results in two types of clouds.

3.1 Evolution of H_2 Inside a Static Cloud

In our first exercise, we assume an interstellar cloud which is static. We start with a spherical molecular cloud having the outer radius at $R_{out} = 1pc$. The outer region of the cloud is assumed to be isothermal at T_{out} where the gas is optically thin. T_{out} is assumed to be a parameter. In this phase, we assume, $\rho \sim r^{-2}$ (Shu, Adams and Lizano, 1987), where r is the radial distance. The accretion rate of H on the grain surface will automatically increase as the density rises. In presence of rotation, centrifugal barrier is formed at $r = r_c$, where the centrifugal force balances gravity. At this stage, the cloud is expected to be disk-like and the opacity becomes high enough to trap radiations. Inside this region, $\rho \propto 1/r$. As a test of our code, we evolve the cloud for ten million years to judge how far inside the cloud the production rate of H is significant.

Biham et al. (2001) pointed out, and we have also verified this to be true, that there

is indeed a narrow temperature range in which the recombination efficiency is the highest. In the case of olivine the peak is at around 7 – 9K and for amorphous carbon the peak is at around 12 – 16K. We chose temperatures at higher side of this peak. In our model calculation we have taken two generic molecular clouds with $R_{out} = 1pc$ and $M = 10M_{\odot}$ and $M = 100M_{\odot}$. We assume the angular velocity of the outer edge of the cloud to be $10^{-16}rad/sec$ so that $r_c = 6.8 \times 10^{14}cm$ and $r_c = 6.8 \times 10^{13}cm$ respectively in these two cases. With these masses, the densities of the gas at the outer edge are $\rho_{out} = 0.162 \times 10^{-21}gm\ cm^{-3}$ and $\rho_{out} = 0.162 \times 10^{-20}gm\ cm^{-3}$ respectively. Densities of the gas at r_c are found out to be $\rho_c = 0.324 \times 10^{-14}gm\ cm^{-3}$ and $\rho_c = 0.262 \times 10^{-11}gm\ cm^{-3}$ respectively. This density is the initial density of the collapsing shell. A notional inflow velocity is provided (which gives an indication of the evolution time to be $t_{ev} \sim r/v$ by assuming a subsonic flow where the sound velocity is given by $a_s \sim (4kT/3m_p)^{1/2}$). In our runs, the velocity is always assumed to be less than this value. We choose $\sim 10^4\ cm/sec$ for concreteness. The activation barrier energies are chosen to be as those of olivine.

The computational procedure involves in dividing the entire cloud into 10^5 shells. We compute the number density in each shell and the mean thermal velocity for temperature $T = T_{out}K$. These enable us to get the accretion rate of H on the grain surface. The rate of desorption of H_2 which controls how much goes back into the gas at each radius is computed. These are normalized by the number density of grains at each radius. We continue our procedure for each shell.

The results presented in this Section are for olivine grains. In Figs. 5a, we present the mass fraction of H and H_2 in the gas phase as a function of the radius of the cloud when $T_{out} = 10K$ when the mass of the cloud is $M = 10M_{\odot}$ (dotted) and $M = 100M_{\odot}$ (solid) respectively. Higher mass clouds produce significant H_2 at much early stage of the evolution since the density is higher. In Fig. 5b, we present the number densities of H and H_2 on the grain surfaces. We remind here that the H_2 values are actually the saturation expectation values at corresponding radii and H values are the corresponding equilibrium values. H_2 goes back to the gas at the rate of R_{H2} (Eq. 3).

In Fig. 6(a-b) we present similar results at $T_{out} = 11K$. The notations and styles are the same as before. Generally speaking, the saturation values of H , H_2 on the grain surfaces increase with decreasing radius as before. Understandably, the production rate is higher when the cloud mass is higher because the accretion rate itself is high. With the rise in temperature, H is not significantly affected, but the production of H_2 in grains and therefore

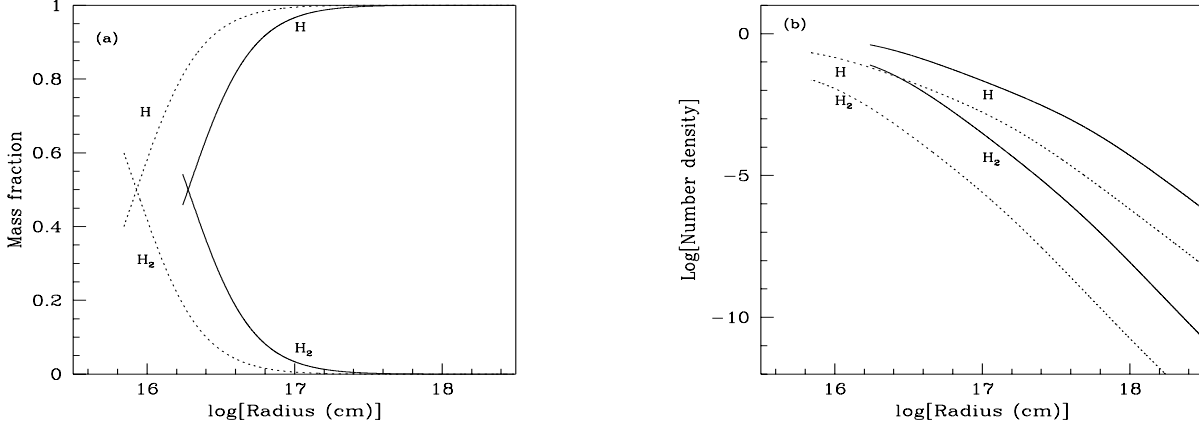


Fig. 5(a-b): Variation of (a) mass fractions of H and H_2 in the gas phase and (b) number densities of H and H_2 on a grain surface with radial distance during the chemical evolution of a static cloud. $T = 10\text{K}$ is assumed. Dotted curves are for $M = 10M_{\odot}$ and the solid curves are for $M = 100M_{\odot}$ respectively. For higher mass cloud the conversion to H_2 is faster because H accretion rate on the grains is higher.

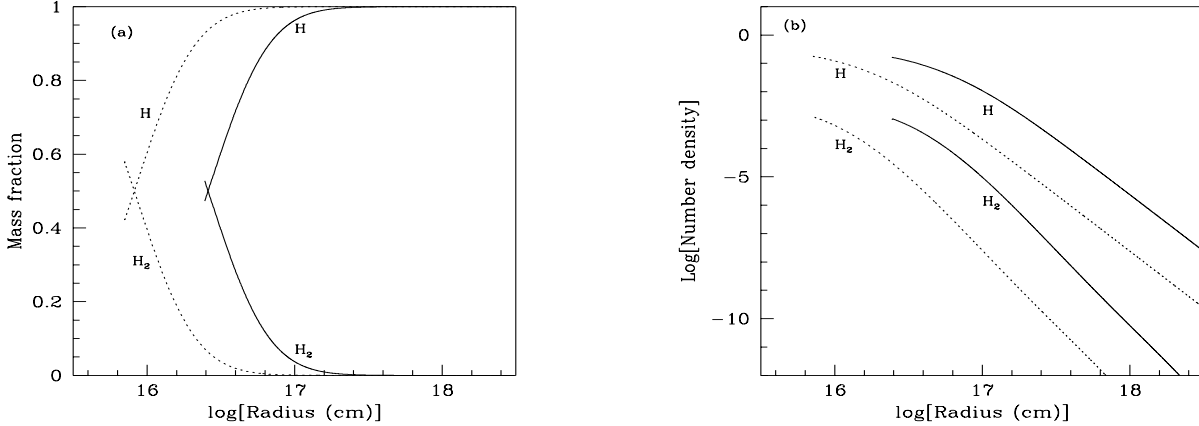


Fig. 6(a-b): Same as Figs. 5(a-b) but the temperature of the gas is $T = 11\text{K}$.

the desorption of H_2 into the gas are dropped. However, as one goes inside, the conversion of H_2 is higher because more H was left over in the gas to increase the accretion rate on grains. As a result, the mass fraction of H_2 crossed 0.5 mark at a larger radius.

3.2 Collapsing Shell

We now compute the variation of H and H_2 with a somewhat different initial condition. We start with a hollow spherical shell which is collapsing. Masses of the shell for two model runs are chosen to be $1M_{\odot}$ and $10M_{\odot}$ respectively. The initial densities are $1.1 \times 10^{-20} \text{ gm cc}^{-1}$ and $1.1 \times 10^{-19} \text{ gm cc}^{-1}$ respectively. The shell thickness is given by 0.0005pc . In order to understand the effect of grain-types and the effect of temperature we choose two sets of

activation energy barriers as presented in Sec. 2.3 above. For each grain type, we choose two temperatures for each of which we run two models with the mass of the shell taken to be $1M_{\odot}$ and $10M_{\odot}$ respectively. Our strategy is to compute the saturation value in this shell and let it collapse into the next shell freely. This becomes the initial condition of the next shell. The evolution proceeds from then on in that shell. The density increases in the same way discussed above while the mass of the shell remains fixed. For clarity, we find it convenient to plot the quantities with time of the collapse. The accretion rate of H on the grains is very high in this model. The resulting number densities of H and H_2 are also large. As a result, H to H_2 conversion is very rapid at early phases of the cloud collapse.

3.2.1 Olivine Shell

First, we choose the activation energy barriers to be those of olivine (see Sec. 2.3). Figure 7a shows the evolution of H and H_2 in the gas phase when the cloud is of mass $M = 1M_{\odot}$ (dotted) and $M = 10M_{\odot}$ (solid) respectively. The temperature of the cloud has been chosen to be $T = 10\text{K}$. Mass fraction of H_2 crosses 0.9 at $t \sim 7.81 \times 10^6\text{yr}$ and $t = 4.7 \times 10^5\text{yr}$ respectively. In Fig. 7b, the number densities on the grain surfaces are plotted. Note that as the conversion to H_2 is rapid (Fig. 7a), the number density of H decreases rapidly in the gas phase. At some point (around $T \sim 10^{5-6}\text{yr}$) the formation H_2 on grains is at a slower rate compared to the desorption rate) and hence the reserve of H_2 on grains goes down. On the other hand, the density of cloud itself increases as the collapse progresses which started increasing the accretion rate towards the end. This increases the number density of the H and H_2 . Thus, in the collapsing shell model the number densities on the grains are lower at the intermediate times.

In Fig. 8(a-b) we repeat the same model (i.e., with the activation barrier energies as those of olivine) but chose the cloud temperature to be slightly higher at $T = 12\text{K}$. The motivation is to show the sensitivity of the final outcome on temperature. The behaviour is similar as in Fig. 7(a-b) except that the mass fraction of H_2 became ~ 0.9 at $t \sim 9.4 \times 10^6\text{Yr}$ and $t \sim 8.1 \times 10^6\text{Yr}$ for $M = 1M_{\odot}$ and $M = 10M_{\odot}$ respectively. This is expected as the recombination efficiency is smaller (see, Fig. 2).

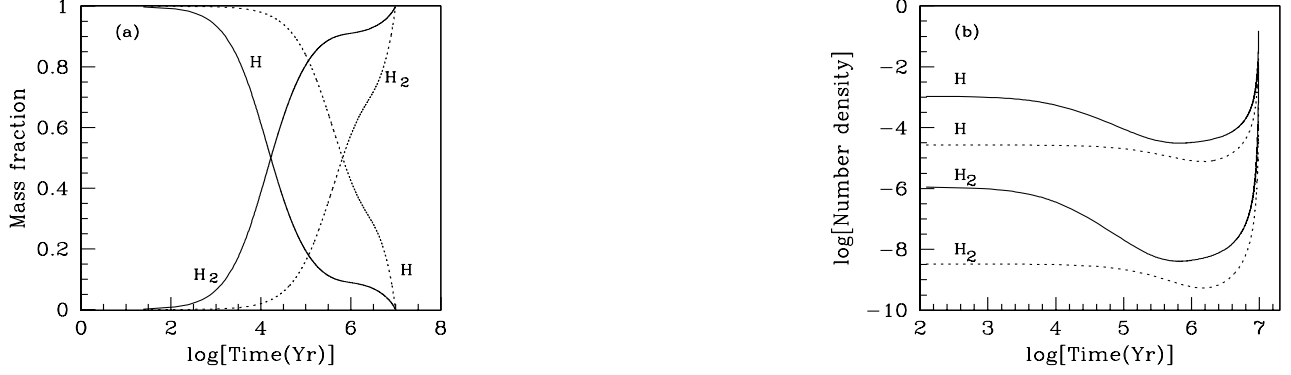


Fig. 7(a-b): Variation of (a) mass fractions of H and H_2 in the gas phase and (b) number densities of H and H_2 on a grain surface with time during the chemical evolution of a collapsing shell. Dotted curves are for $M = 1M_{\odot}$ and the solid curves are for $M = 10M_{\odot}$ respectively. Mass fraction of H_2 reaches ~ 0.9 in a matter of 7.8×10^6 yr and 4.7×10^5 yr for low and high mass shells respectively.

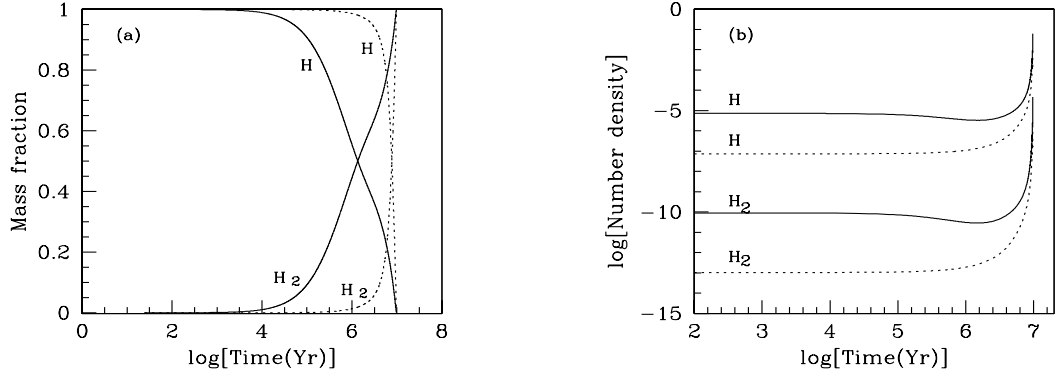


Fig. 8(a-b): Same as in Fig. 7(a-b) but the temperature of the cloud is assumed to be 12K. Mass fraction of ~ 0.9 is achieved by H_2 in a matter of 9.4×10^6 yr and 8.1×10^6 yr for low and high mass shells respectively.

3.2.2 Amorphous Carbon Shell

We now assume the activation barrier energies chosen to be those of amorphous carbon grains. In this case, it is possible to go to higher temperatures. We run at two temperatures, $T = 20$ K and $T = 25$ K respectively for the shells of $M = 1M_{\odot}$ and $M = 10M_{\odot}$ respectively. In Figs. 9(a-b), we plot the results for $T = 20$ K. Here, the plot characteristics remained the same as before. The mass fraction of H_2 reaches 0.9 at $t = 9.1 \times 10^6$ and $t = 6.4 \times 10^6$ yr for low and high mass shells respectively.

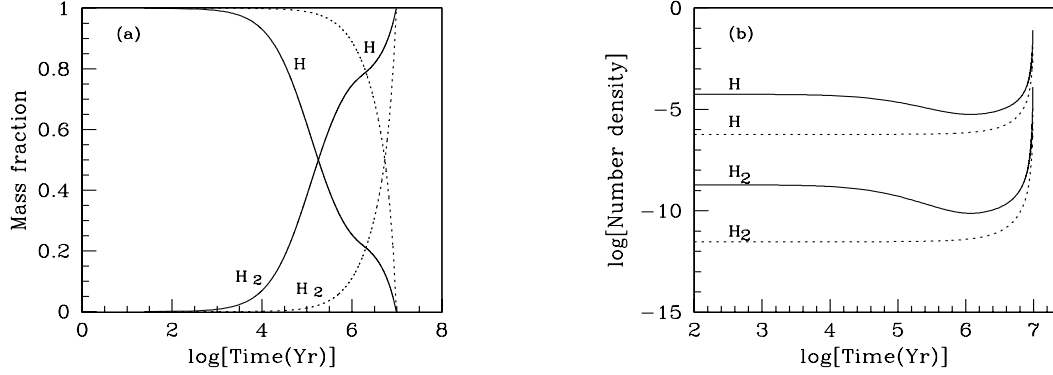


Fig. 9(a-b): Same as in Fig. 7(a-b) but the activation barrier energies of the cloud is assumed to be those of amorphous carbon. The temperature is chosen to be $T = 20\text{K}$. Mass fraction of ~ 0.9 is achieved by H_2 in a matter of $9.1 \times 10^6\text{yr}$ and $6.4 \times 10^4\text{yr}$ for low ($M = 1M_{\odot}$) and high ($M = 10M_{\odot}$) mass shells respectively.

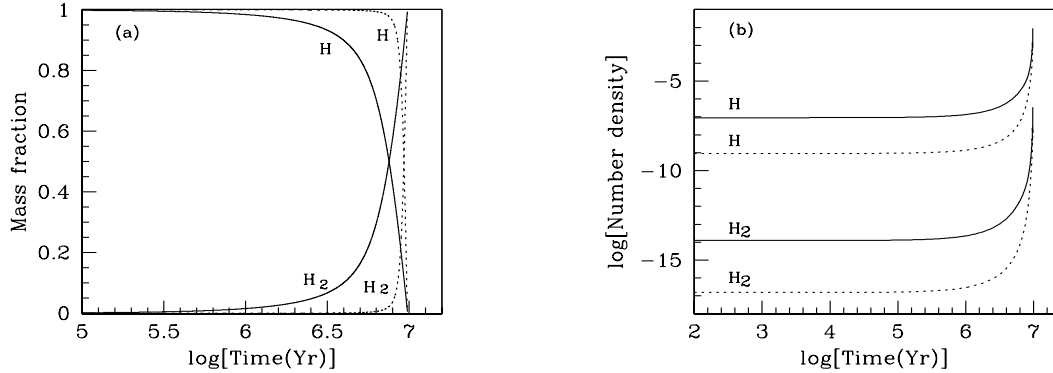


Fig. 10(a-b): Same as in Fig. 8(a-b) but the temperature of the cloud is assumed to be 25K . Mass fraction of ~ 0.9 is achieved by H_2 in a matter of $9.5 \times 10^6\text{yr}$ and $9.36 \times 10^6\text{yr}$ for low ($M = 1M_{\odot}$) and high ($M = 10M_{\odot}$) mass shells respectively.

years for $M = 1M_{\odot}$ and $M = 10M_{\odot}$ respectively. In Fig. 9b, we show the number densities of H and H_2 on grains. Here too, there is a minimum at an intermediate time. Similar Figures as above for $T = 25\text{K}$ are plotted in Figs. 10(a-b) and the mass fraction of H_2 reached 0.9 at $t = 9.5 \times 10^6\text{yr}$ and $t = 9.36 \times 10^6\text{yr}$ respectively. Thus, in the case of higher activation energy, the sensitivity of the final result on the shell mass is weaker.

In this context, we wish to mention that while computing the formation of H_2 using a constant surface reaction rate supplied by UMIST database (Millar et al. 1997) it was

observed that most of the H is converted to H_2 at a somewhat later stage (Chakrabarti & Chakrabarti, 2000), at least after 10^7 yr of the beginning of the collapse. Our work with computation with up to date grain surface chemical processes indicates that the conversion is perhaps faster. In future, we shall compute more complex molecules and would compare them with observed tabulated value (e.g. Herbst 1992 and van Dishoeck et al. 1993).

4 DISCUSSION AND CONCLUDING REMARKS

In this paper, we studied evolution of molecular hydrogen in the gas phase and on the grain surface in two toy models, namely, in (a) a static interstellar cloud and (b) the collapsing phase of a spherical shell. In the later case, we chose two different types of activation barrier energies which correspond to olivine and amorphous carbon grains. Instead of using the complete grain size distribution, we assumed three major grain sizes where there are humps in the WD distribution. We compared the results from the rate and the master equation for each type of grains and determined the applicability of these equations as a function of the accretion rate of H on grains. Using static and collapsing shell models with prescribed density, temperature and velocity distributions, we showed how gradually H_2 builds up in the grain and the gas. Earlier, using a constant and representative surface reaction rates given in the UMIST data base for H to H_2 conversion, it was shown that the conversion process is slower (e.g. reaching mass fraction of ~ 0.5 after $t \sim 10^7$ yr). However, here we find that ninety percent conversion to H_2 is achieved in a matter of $10^5 - 10^7$ years depending on cloud parameters such as activation energy and temperature of the grains, and the mass of the cloud. In terms of spatial distribution, we find that most of the conversion takes place for a radial distance $r > 0.1$ pc, i.e., at the outer shell of the molecular cloud.

In our work, we chose simple power-law density distribution inside an isothermal cloud. Li and Draine (2001) considered the effect of radiations on the grains in diffused interstellar clouds and computed the grain temperature as functions of grain size distribution. They also computed the resulting infrared spectra. Recent numerical solutions of several workers such as Galli, Walmsley & Goncalves (2002), Zucconi, Walmsley & Galli (2001) have shown that dust temperature inside the dense cloud could be as low as 6K and the temperatures of the gas and grain become roughly identical when the gas density $n \gtrsim \text{few} \times 10^4 \text{ cm}^{-3}$. Thus our assumption of the equality of the grain and the dust temperatures may be justified since our number densities are of this order or higher. On the other hand, COBE/DIRBE

results (e.g., Lagache et al. 1998) do not seem to support the existence of very cold dusts. We therefore chose the cloud temperature at 10K and above.

Our work concentrated on the gravitational collapse of a dense cloud induced by Jean's instability. In a different context, Bergin et al. (2004) studied the evolution of the molecular hydrogen inside an extremely diffused cloud the formation of which is induced by the passage of a shock wave. The temperatures used were very high (reaching several thousand) which is appropriate for such a cloud of very low extinction. In their work, though the gas-grain interaction was simplified through by using a production rate of H_2 as given in Millar, Farquhar, Willacy (1997), they used destruction of H_2 through cosmic rays and UV radiation. They also studied the formation rate of CO molecule.

In our paper, we have thoroughly dealt with the most basic surface chemistry, namely the H_2 formation deep inside a cold, dense cloud. In future, we shall apply our procedure to include diffused clouds at high temperatures following above work and explore the possibility of formation of more complex molecules and especially the formation of bio-molecules during the collapse phase.

ACKNOWLEDGMENTS

The authors thank the referee for very useful comments leading to improvements in the manuscript. This work is supported in part by Indian Space Research Organization (ISRO) Grant from a RESPOND project.

REFERENCES

- Acharyya, K., Chakrabarti, S. & Chakrabarti, S.K., 2002, in Proceedings of XIIth National Space Science Symposia, (Ed.) A.K. Gwal, p. 380
- Acharyya, K., Chakrabarti, S. & Chakrabarti, S.K., 2004, Ind. J. Phys. 78(B) 7
- Bergin, E.A., Hartmann, L.W., Raymond, J.C. & Ballesteros-Paredes, J. 2004 astro-ph/04005329
- Biham, O., Furman, I., Pirronello, V., and Vidali, G., 2001, ApJ 553, 595
- Cazaux, S. and Tielens, A.G.G.M., 2002, ApJ 575, L29
- Cazaux, S. and Tielens, A.G.G.M., 2002, ApJ 604, 222
- Chakrabarti, S. and Chakrabarti, S. K., 2000, A & A 354, L6
- Galli, D., Walmsley, M. & Goncalves, J., 2002, A & A, 394, 275
- Gould, R. J. and Salpeter, E. E., 1963, ApJ 138, 393
- Green, N.J.B, Toniazzo, T., Pilling, M.J., Ruffle, D.P., Bell, N. & T.W. Hartquist, 2001, A&A, 375, 1111
- Hartmann, L., 1998, Accretion Processes in Star Formation (Cambridge Univ. Press:UK)
- Hasegawa, T. and Herbst, E., 1993, MNRAS 261, 83
- Hasegawa, T. I., Herbst, E. and Leung, C. M., 1992, ApJS, 82, 167

- Herbst, E., 1992, *The Production of Large Molecules in Dense Interstellar Clouds in Chemistry and Spectroscopy of Interstellar Molecules* (Tokyo: Univ of Tokyo Press)
- Hollenbach, D. and Salpeter, E. E., 1971, ApJ 163, 155
- Hollenbach, D., Werner, M.W. and Salpeter, E. E., 1971, ApJ 163, 165
- Katz, N., Furmann, I., Biham, O., Pironello, V. and Vidali, G., 1999, ApJ 522, 305
- Lagache, G., Abergel, A., Boulanger, F. and Puget, J.-L., 1998, A & A, 709
- Leung, C. M., Herbst, E. and Huebner, W. F., 1984, ApJS 56, 231
- Li, A. & Draine, B., 2001, ApJ, 554 778
- Lipshtat, A., Biham, O. and Herbst, E., 2004, 348, 1055
- Mathis, J. S., Rumpl, W. and Nordsieck, K. H. 1977, ApJ 217, 425 (MRN)
- Millar, T.J., Farquhar, P. R. A. and Willacy, K., 1997, A & A Suppl. Ser. 121 139
- Prasad, S. S. and Huntress, W.T. 1980a, ApJS, 43, 1
- Prasad, S. S. and Huntress, W.T. 1980b, ApJ, 239, 151
- Rae, J.G.L., Green, N.J.B., Hartquist, T.W., Pilling, M.J. and Toniazzi, T. A&A, 405, 387
- Shu, F. H., Adams, F. C. and Lizano, S., 1987, ARAA 25, 23
- Stantcheva, T., Shematovich, V.I., Herbst, E. 2002, A&A, 391, 1069
- van Dishoeck, E., Black, G., Draine, B. T., Lunine, J.I., 1993, *Protostars and Planets-III* Eds. E. H. Levy, J. I. Lunine and M. S. Matthews (Arizona: Univ. of Arizona Press) 163
- Weingartner, J. C. and Draine, B. T., 2001a, ApJS 134, 264
- Weingartner, J. C. and Draine, B. T., 2001b, ApJ 548, 296 (WD)
- Zucconi, A., Walmsley, M. & D. Galli, 2001, A & A, 376, 650